Acta Pharmaceutica Sinica B 2025;15(6):3059−3072

Chinese Pharmaceutical Association
Institute of Materia Medica, Chinese Academy of Medical Sciences

Acta Pharmaceutica Sinica B

www.elsevier.com/locate/apsb
www.sciencedirect.com

ORIGINAL ARTICLE

RBM14 enhances transcriptional activity of p23 regulating CXCL1 expression to induce lung cancer metastasis

Wen Zhang[a,b,c,†], Yulin Peng[b,†], Meirong Zhou[a,c,†], Lei Qian[d,†], Yilin Che[a], Junlin Chen[a], Wenhao Zhang[a], Chengjian He[a], Minghang Qi[c], Xiaohong Shu[c], Manman Tian[a], Xiangge Tian[a], Yan Tian[c], Sa Deng[c], Yan Wang[b], Xiaokui Huo[a,*], Zhenlong Yu[c,*], Xiaochi Ma[a,b,*]

[a]*Second Affiliated Hospital, Dalian Medical University, Dalian 116000, China*
[b]*Dalian Key Laboratory of Metabolic Target Characterization and Traditional Chinese Medicine Intervention, College (Institute) of Integrative Medicine, Dalian Medical University, Dalian 116044, China*
[c]*College of Pharmacy, Dalian Medical University, Dalian 116044, China*
[d]*Advanced Institute for Medical Sciences, Dalian Medical University, Dalian 116044, China*

Received 25 October 2024; received in revised form 25 January 2025; accepted 3 March 2025

KEY WORDS

Lung cancer;
Epithelial−mesenchymal transition;
Invasion and metastasis;
RNA-binding motif protein 14;
Prostaglandin E synthase 3;
CXCL1;
Transcriptional regulation;
Protein−protein interaction

Abstract Metastasis serves as an indicator of malignancy and is a biological characteristic of carcinomas. Epithelial−mesenchymal transition (EMT) plays a key role in the promotion of tumor invasion and metastasis and in the enhancement of tumor cell aggressiveness. Prostaglandin E synthase 3 (p23) is a cochaperone for heat shock protein 90 (HSP90). Our previous study showed that p23 is an HSP90-independent transcription factor in cancer-associated inflammation. The effect and mechanism of action of p23 on lung cancer metastasis are tested in this study. By utilizing cell models *in vitro* and mouse tail vein metastasis models *in vivo*, the results provide solid evidence that p23 is critical for promoting lung cancer metastases by regulating downstream CXCL1 expression. Rather than acting independently, p23 forms a complex with RNA-binding motif protein 14 (RBM14) to facilitate EMT progression in lung cancer. Therefore, our study provides evidence for the potential role of the RBM14−p23−CXCL1−EMT axis in the metastasis of lung cancer.

*Corresponding authors.
E-mail addresses: huoxiaokui@163.com (Xiaokui Huo), qdyuzl871123@163.com (Zhenlong Yu), maxc1978@163.com (Xiaochi Ma).
[†]These authors made equal contributions to this work.

Peer review under the responsibility of Chinese Pharmaceutical Association and Institute of Materia Medica, Chinese Academy of Medical Sciences.

https://doi.org/10.1016/j.apsb.2025.03.048

1. Introduction

Lung cancer has become a prominent contributor to global mortality rates associated with malignancies and is a major global public health burden[1-3]. Despite advancements in diagnosis, surgical techniques, radiotherapy, and chemotherapy over the past decade[4-6], the mortality rate of lung cancer remains alarmingly high, with a mere 15% 5-year survival rate, primarily due to the widespread metastasis of lung cancer[7,8]. The efficacy of targeted therapy in tumor treatment is promising. However, the intricate interactions between the tumor and its stroma greatly impede the development of targeted therapies for tumor metastasis. Therefore, it is imperative to investigate novel molecular mechanisms and targets of lung cancer metastasis to establish a theoretical foundation for developing innovative treatment strategies or therapeutic agents and ultimately enhance the quality of life for patients with lung cancer.

The process of epithelial−mesenchymal transition (EMT) in tumor cells is characterized by the loss of intercellular adhesion among epithelial tumor cells and the acquisition of migration and invasion properties of mesenchymal cells, thereby promoting the metastasis and development of various cancers[9]. The acquisition of metastatic properties by tumor cells increased aggressiveness, bringing substantial challenges to clinical management and patient survival[10]. Therefore, there is an urgent need to investigate the molecular targets and pathways involved in EMT in tumor cells, which will not only establish a theoretical foundation for preventing EMT but also facilitate the identification of potential therapeutic agents. In the present study, we focus on the EMT marker, CXCL1, to reveal a new mechanism for the regulation of its expression.

CXCL1, a chemokine of the CXC family, is implicated in the pathogenesis of various inflammatory diseases and plays a crucial role in physiology and cancer progression, particularly in EMT[11-13]. Elevated CXCL1 expression in tumor tissues and serum has been associated with tumor metastasis and poor prognosis in ovarian cancer, lung adenocarcinoma, colorectal cancer, and pancreatic ductal adenocarcinoma[14-18]. A previous study reported that CXCL1 is positively correlated with the migration and invasive activity of osteosarcoma cell lines[19] and has become a key indicator of lung metastasis in osteosarcoma through paracrine release. Therefore, it was proposed that the targeted inhibition of CXCL1 could exert a profound inhibitory effect on tumor growth and metastasis.

Prostaglandin E synthase 3 (p23) is a highly conserved protein encoded by the *PTGES3* gene[20,21], which is often overexpressed in various cancers, including prostate cancer, breast cancer, and lung cancer[22-27]. The current understanding of p23 mainly focuses on its role as a co-partner of heat shock protein 90 (HSP90)[28,29]. It can stabilize the complex formed by HSP90 and its client proteins, including the estrogen receptor[30], androgen receptor[31], and telomerase[32]. However, p23 can also perform some functions independent of HSP90, such as enhancing the transcription factor activity of p53[33] and protecting human aryl hydrocarbon receptors from degradation[34]. Our previous study redefined p23 as an HSP90-independent transcription factor of prostaglandin G/H synthase 2 (COX-2) that promotes tumor growth[35]. This highlights the diversity and complexity of p23 functionality and emphasizes the importance of further studies on its functional characteristics. Currently, there are few studies on p23 expression and tumor metastasis. Therefore, it is important to explore the role of p23 in tumor migration and its underlying molecular mechanisms.

RNA-binding motif protein 14 (RBM14) is an RNA-binding protein with a low-complexity domain that is divided into 2 subtypes. Among them, subtype I acts as a nuclear receptor coactivator, enhancing transcription through other coactivators, such as NCOA6 and CITED1, whereas subtype II acts as a transcription inhibitor, regulating the transcriptional activity of coactivators, including subtype I RBM14, NCOA6, and CITED1[36]. It has been reported[37] that the depletion of RBM14 in human cells induces the ectopic formation of acentrosomal protein complexes by affecting the function of the STIL/CPAP complex, and this abnormal structure may lead to genomic instability and tumorigenesis. In terms of tumor metastasis, it is reported in the literature[38] that RBM14 can stimulate the phenotypic polarization of liver macrophages (M2), thus promoting the malignant invasion of liver cancer cells both *in vitro* and *in vivo*. Another study[39] reported that SLC35F2 (a member of the solute carrier family) regulates the invasion, metastasis, and cisplatin resistance of pancreatic cancer cells by regulating the expression of RBM14. In addition, RBM14 plays an important role in DNA double-stranded break repair[40,41]. However, the mechanism of action of RBM14 and its interacting proteins in the process of tumor metastasis remains unclear and requires further study.

In this study, we discovered a novel function of p23 as a transcription factor that promotes EMT in lung cancer, and we revealed its specific mechanism. Its activation of the CXCL1 promoter is not achieved directly but requires the assistance of the cofactor RBM14 during EMT progression.

2. Materials and methods

2.1. Reagents and antibodies

CXCL1 was purchased from Sigma (St Louis, MO, USA) with >98% purity. It was dissolved in water containing 5% bovine serum albumin, and the concentration of the stock solution was 25 mmol/L, which was stored at −80 °C. Purified p23 and RBM14 were obtained from Invitrogen (Carlsbad, CA, USA). Anti-HA tag antibodies were procured from Cell Signaling Technology (Danvers, MA, USA). Primary antibodies against p23, Flag, RPS3, vimentin, HNRNPU, β-actin, DDX5, and secondary antibodies were all purchased from Proteintech Group (Chicago, IL, USA). AbClonal Technologies (Wuhan, China) provided the primary antibodies against CXCL1 and RBM14. Jingjie PTM BioLab (Hangzhou, China) provided primary antibodies against E-cadherin and N-cadherin. Fetal Bovine Serum (FBS), Dulbecco's modified Eagles' medium (DMEM), RPMI 1640, trypsin and were purchased from HyClone Laboratories (Logan, UT, USA). The other chemicals were all obtained from Sigma Chemical Co. (St. Louis, MO, USA).

2.2. Cell lines and cell culture conditions

The cell lines from human lung cancer (A549, H1299, H322, H460, and HCC827), HLF, and HEK-293T cells were obtained from the American Type Culture Collection (Manassas, VA, USA) or the Procell Life Science & Technology Co. (Wuhan, China) and were maintained in our laboratory. The cells were cultivated in F12K, DMEM, or 1640 medium, which were enriched with 10% FBS, 100 μg/mL streptomycin and 100 μg/mL penicillin at 37 °C within a humidified atmosphere containing 5% CO_2.

2.3. Cell migration assay

The migration of cells was measured using CIM plates, with 1×10^5 cells per well. The cells were cultivated at 37 °C in an atmosphere containing 5% CO_2. Migration curves of cells were recorded using the xCELLigence system (Roche Applied Sciences, Basel, Switzerland) all the time.

2.4. Lentivirus preparation and transfection

We used a second-generation packaging system to produce lentivirus in 293T cells. This system contains plasmids $psPAX_2$ (Addgene, MA, USA) and pMD2.G (Addgene). For transfection, a 100 mm culture dish containing 4×10^6 293T cells was used with 7.5 μg $psPAX_2$ and 7.5 μg pMD2.G using Lipofectamine 2000 (Invitrogen). After transfection for 48 h, the supernatant was collected and then concentrated with PEG-8000, and virus titers were determined by serial dilution. Infection multiplicities during transfection were five.

2.5. RNA interference and transfection

The target sequences of p23 siRNAs (GenePharma, Shanghai, China) are as follows:

1. 5′-CCAAAUGAUUCCAAGCAUATT-3′
2. 5′-GGCUUAGUGUCGACUUCAATT-3′
3. 5′-GUCAGUGUUCCAGGUGUAUTT-3′

The target sequences of RBM14 siRNAs (Sangon, Shanghai, China) were as follows:

1. 5′-CGCGUUUGUUCACAUGGAGAATT-3′
2. 5′-CCCAAGCAUCAAUGGGCCUUUTT-3′

2.6. Immunohistochemical staining of tissue microarray

Samples of cancer tissue in tissue microarray were obtained from Shanghai Outdo Biotech Company (Ethical No. SHYJS-CP-1701003), and written informed consents were obtained from all participants. Briefly, paraffin sections of 4−6 μm were deparaffinized and rehydrated with xylol and a descending series of alcohol solutions. A 3% hydrogen peroxide solution was used to stop the body's natural peroxidase activity for 20 min. The sections were then retrieved using 10 mmol/L citrate buffer (pH 6.0) in a microwave for 20 min. Sections were subsequently incubated with primary antibodies overnight at 4 °C in a humidified box. The next day, the samples were left with the right biotinylated secondary antibodies for 1 h at room temperature. Sections were counterstained with hematoxylin, dehydrated using a series of increasing concentrations of alcohol and xylene, and sealed with coverslips. Images were taken under a light microscope (20 × magnification).

2.7. Cell Transwell assay

Cells were resuspended in 100 μL of serum-free medium and seeded in the upper chamber of the Transwell chamber plates (BD Biosciences, NJ, USA). The bottom well contained 15% FBS. After 48 h of growth at 37 °C, the cells that had moved through the holes in the Transwell were fixed and stained with crystal violet.

2.8. Wound healing assay

Cells were seeded in 6-well plates and formed confluent monolayers overnight. Then, the wounds were created by scratching lines across the surface using a 10 μL plastic pipette tip. The wounds were recorded by a microscope after 0 and 48 h.

2.9. RT-PCR

Total RNA was extracted from the cells using the TRIzol reagent (Invitrogen). The preparation of the cDNA was done by Quantscript RT Kits (MonAmp, Wuhan, China) with oligo(dT) or random primers. For transcript quantification using specific primers, a SYBR RT-PCR kit (MonAmp) was used. The $2^{-\Delta\Delta Ct}$ method was employed to quantify expression levels. The primers that were used are enumerated in Supporting Information Table S1. For cancer tissues detection, the samples were obtained from Second Affiliated Hospital of Dalian Medical University (Ethical No. KY2022-173), and written informed consents were obtained from all participants.

2.10. Nuclear and cytoplasmic protein extraction

The collected cell precipitate was resuspended in reagent buffer A (containing 0.5 mmol/L $MgCl_2$, 5 mmol/L KCl, 25 mmol/L HEPES, protease inhibitor) and lysed on ice for 30 min. The supernatant, which contained cytoplasmic proteins, was then centrifuged at 4 °C for 10 min. For the extraction of nuclear proteins, reagent buffer B (containing 25 mmol/L HEPES, glucose powder, 400 mmol/L NaCl, protease inhibitor) was added to the precipitate obtained in the previous step. The supernatant contained the nuclear proteins after centrifugation.

2.11. Western blot

Cells were lysed in RIPA buffer, and supernatants were collected at 12,000×*g* for 10 min at 4 °C by centrifugation. The BCA detection kit was used to determine protein levels. Sodium dodecyl sulphate-polyacrylamide gel electrophoresis was performed after boiling. Proteins were separated by molecular weight and were transferred to a 0.45 μm PVDF membrane. Corresponding antibodies were incubated overnight at 4 °C in a refrigerator after blocking with 5% milk. Secondary antibodies were incubated at room temperature for 1 h and were detected by enhanced chemiluminescence or the ODYSSEY CLX system (Licor, Lincoln, NE, USA).

2.12. Transcriptome sequencing and analysis

RNA was separated and purified according to the type of RNA detected after total RNA was extracted from the samples. RNA was fragmented to the length required by the sequencing platform (or fragmented after reverse transcription). Sequencing linkers were then added. PCR amplification was carried out to achieve a

certain level of abundance, and sequencing was carried out until a sufficient number of sequences had been obtained. To generate a genome-wide transcription profile, the sequences were compared to the reference genome or assembled *de novo*. The differentially expressed genes were identified as potential target genes of p23 by comparing three groups of A549 cell lines with p23 knockdown and blank A549 cells.

2.13. Streptavidin-agarose pulldown assay

A 541 bp biotin-labeled double-stranded probe corresponding to the sequence of the CXCL1 promoter (−541 to +38 bp) was synthesized. Briefly, 500 μg protein, 4 μg DNA probe, 40 μL streptavidin-conjugated agarose beads, and 1 × phosphate-buffered saline (PBS) buffer with 1 mmol/L DTT and 1 mmol/L EDTA were incubated at 25 °C for 6 h on a rotary plate. Beads were resuspended in a loading buffer and boiled at 100 °C after washing with PBS buffer. Then, a Western blot analysis of the supernatant was performed.

2.14. Dual-luciferase reporter gene assay

The luciferase activity was measured using a dual luciferase reporter assay system (Promega, Madison, WI, USA). Cells in the 6-orifice plate were collected and lysed. Subsequently, 10 μL of lysate was transferred into a black 96-well plate (Thermo, Waltham, MA, USA). Cell lysates from each well were assayed sequentially for firefly and *Renilla* luciferase activity.

2.15. Electrophoretic mobility shift assay (EMSA)

BGI Genomics (Beijing, China) provided biotin-labelled CXCL1 promoter probes. For the EMSA assay, 4 μg of protein and 1 μg of the biotin-labelled DNA probe were mixed in binding buffer and incubated for 20 min at 25 °C. DNA−protein complexes were separated on 6.5% acrylamide-native PAGE gels at 4 °C. Specific bands were detected using horseradish peroxidase-conjugated streptavidin and enhanced chemiluminescence.

2.16. Immunoprecipitation (IP)

In total, 800 μg of protein was used, and the volume was made up to 500 μL with binding buffer. Subsequently, 2 μg of Flag antibody was included in the experimental group, and 2 μg of IgG antibody was included in the blank group. The samples were vortexed for 1 h. After the vortex, 15 μL magnetic beads were added and vortexed overnight at 4 °C. Magnetic separation was performed the next day, adding a suitable amount of binding buffer for washing the magnetic beads three times after discarding the supernatant. 50 μL of 2 × loading buffer was added to the beads and allowed to boil for 10 min. The supernatant was collected for Western blot analysis after magnetic separation.

2.17. Animal experiments

Five-week-old male NYG mice were bought from Beijing Vital River Laboratory Animal Technology Co., Ltd. (Beijing, China) and maintained at the SPF Laboratory Animal Facility of Dalian Medical University (Ethical No. AEE19048). Animals were given sterilized water and food. They were acclimated for 10 days and randomly divided before the experiments. The specified tumor cells (1×10^6 in 100 μL PBS) were injected into the tail vein of each mouse. Four weeks after injection, the lungs were excised, and the number of pulmonary metastatic nodules was counted. Sections of pulmonary metastatic tissue were stained with hematoxylin and eosin (H&E). All procedures were carried out according to the recommendations of the Animal Care and Ethical Committee of Dalian Medical University (Dalian, China).

2.18. Statistical analysis

Statistical analyses were performed using GraphPad 8.0. Kaplan−Meier method was used for survival analysis. The results were presented as mean ± standard deviation (SD). Correlations between histochemical markers were assessed using Pearson's correlation test. The unpaired Student's *t*-test was used for the evaluation of differences between two groups. Any differences where $P < 0.05$ were considered to be statistically significant.

3. Results

3.1. p23 expression is upregulated in lung cancer exhibiting metastatic features

To evaluate the potential involvement of p23 in the metastasis of lung cancer, we queried the Cancer Genome Atlas Program (TCGA) and found that p23 expression was markedly upregulated in metastatic lung cancer compared to primary lung cancer (Fig. 1A), which was further confirmed in clinical samples by immunohistochemical staining (Fig. 1B), qPCR assays (Fig. 1C), and Western blot (Fig. 1D). We investigated p23 expression and prognostic significance in 93 patients with lung adenocarcinoma. Elevated p23 expression promoted metastatic spread of lung cancer (Fig. 1E) and decreased overall survival of patients with metastatic lung cancer (Fig. 1F). These results suggest that increased p23 expression may be associated with metastasis and may predict poor clinical outcomes in patients with metastatic lung cancer.

3.2. Knocking down p23 inhibits the invasion and migration of lung cancer cells

To identify the potential mechanisms underlying the role of p23 in metastasis, we first investigated the expression of p23 in different cell lines, as shown in Supporting Information Fig. S1A. Then we constructed p23 stable knockdown cells using three different p23 knockdown sequences in the A549 cell line (Fig. S1B), and evaluated their impacts on the migratory and invasive capabilities of lung cancer cells. Real-time analysis using the xCELLigence system provided compelling evidence that the migratory ability of A549 lung cancer cells was impaired by depletion of endogenous p23 (Fig. 1G). Similar results were obtained in the scratch assay (Fig. 1H, Fig. S1C), Transwell invasion assays (Fig. 1I, Fig. S1D), and migration assays (Fig. 1J, Fig. S1E). In addition, several proteins involved in EMT were also evaluated using Western blot (Fig. 1K) and qPCR analysis (Fig. 1L), which demonstrated that the knockdown of p23 (shp23) markedly reduced the protein levels of N-cadherin and vimentin, while concurrently leading to an increase in E-cadherin. By contrast, stable p23 overexpression (H1299/OEp23) promoted metastasis in H1299 lung cancer cells (Fig. S1F−S1I). Furthermore, a mouse model of lung cancer metastasis was established. Tumor cells were injected intravenously into the tail vein to evaluate the effect of p23 on metastasis

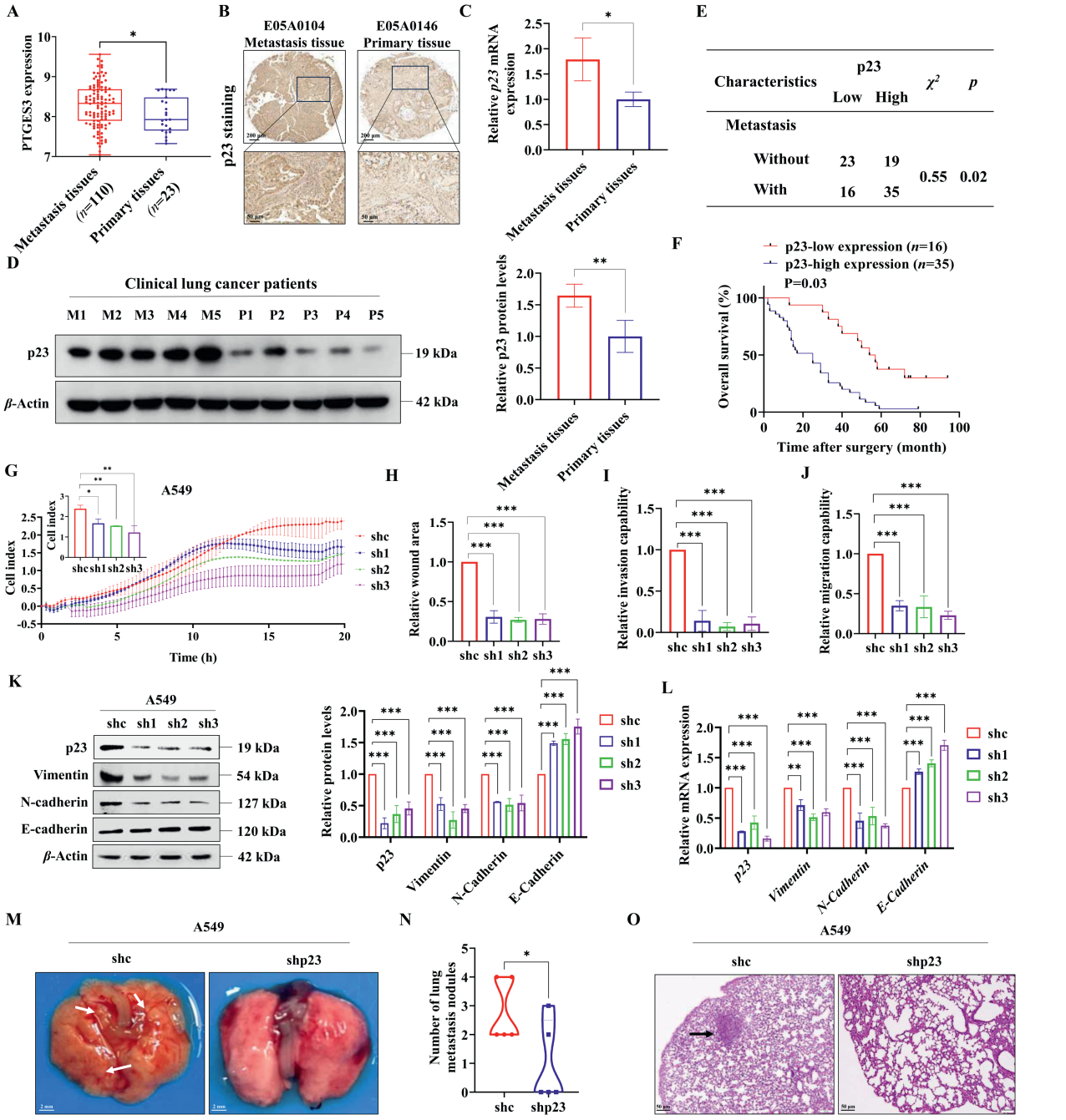

Figure 1 p23 expression is upregulated in lung cancer exhibiting metastatic features. (A) TCGA clinical database analysis of the disparity in the expression of p23 between lung cancer tissues with lymph node metastasis and those without. (B) Representative immunohistochemical staining images. Scale bar: 200 μm (upper panel) and 50 μm (lower panel). (C) Relative mRNA levels of *p23*, $n = 5$. (D) Representative Western blotting images of p23, and quantitative analysis were performed using image lab software, $n = 5$. (E) Microarray analysis of the relationship between lung cancer metastasis and p23 expression. (F) Overexpression of p23 causing lung cancer metastasis decreased disease-free survival in lung cancer patients. (G) xCELLigence assay monitored the number of migrating cells, $n = 3$. (H) The wound healing assay tested the migration ability of cells, $n = 3$. (I, J) The Transwell invasion assay (I) and migration assay (J) determined the number of migrating cells. $n = 3$. (K) Relative mRNA levels of migration and invasion-related genes after p23 knockdown, $n = 3$. (L) Representative Western blotting images of migration and invasion-related proteins after p23 knockdown, and quantitative analysis were performed using image lab software, $n = 3$. (M) Representative lung metastatic nodule images after tail vein injection of A549/shc or A549/shp23 cells. Scale bar: 2 mm, $n = 5$. (N) Statistics of lung metastatic nodule numbers in each group, $n = 5$. (O) Representative H&E staining images for lung metastatic nodules. Scale bar: 50 μm, $n = 3$. Results are presented as mean ± SD. $^*P < 0.05$, $^{**}P < 0.01$, $^{***}P < 0.001$ denotes a significant difference between the groups.

in vivo. Consistent with *in vitro* observations, shp23 dramatically decreased the number of metastatic lung nodules (Fig. 1M−O). These data suggest an oncogenic role for p23 in the promotion of lung cancer metastasis.

3.3. Downstream target gene CXCL1 of p23 was identified by RNA-sequencing

To determine the molecular pathways involved in p23-driven lung cancer metastasis. Transcriptome sequencing on the three p23 knockdown groups was performed to explore potential target genes related to p23 (Fig. 2A). The 3 p23 knockdown groups shared a total of 94 differentially expressed genes (Fig. 2B). These 94 candidates differentially expressed genes were selected for KEGG pathway enrichment analysis (Fig. 2C). The analysis revealed enrichment in signaling pathways, such as IL-17, TGF-β, and NF-κB, marked by genes, including *CXCL1*, *CXCL8*, S100A9 and so on, suggesting a correlation between p23 knockdown and EMT. Analysis of typical lung cancer EMT marker genes from the EMT database (www.EMTome.org) (Fig. 2D) highlighted 6 genes (*CXCL1*, *CXCL8*, *FST*, *PLIN2*, S100A9, and *PRODH*) within KEGG signaling pathways. These genes were subsequently confirmed by qPCR (Fig. 2E), which also confirmed the findings of the RNA-seq analysis. Moreover, we observed that proteins, such as S100A9 and PRODH, showed higher differential expression between the control and p23 knockdown groups, however, their absolute expression levels were relatively low in A549 cells (Fig. 2F). Considering the fold changes and absolute expression levels, CXCL1 was selected as a potential downstream factor of p23.

CXCL1 is a vital chemokine driver that promotes tumor metastasis[14,19,42]. We propose that p23 is involved in lung cancer metastasis, at least in part, by regulating CXCL1 expression. Importantly, both p23 and CXCL1 expression were found to be significantly upregulated in metastatic lung cancer tissues compared to non-metastatic counterparts at both mRNA and protein levels (Fig. 2G and H). In addition, CXCL1 expression was significantly downregulated by p23 depletion and upregulated by p23 overexpression at both the mRNA and protein levels in lung cancer cells (Fig. 2I−L), suggesting that p23 regulates CXCL1 expression in lung cancer cells.

3.4. EMT induced by p23 is partially dependent on CXCL1

In order to test whether p23 achieves its metastatic regulatory functions in a way that depends on the presence of CXCL1, we generated H1299/shCXCL1 lung cancer cells stably overexpressing p23 (H1299/shCXCL1+OEp23) to detect alterations in EMT. As shown in Supporting Information Fig. S2A and S2B. CXCL1 knockdown largely diminished lung cancer cell invasion and migration *in vitro*, and p23 overexpression rescued the lung cancer metastasis reduction induced by CXCL1 knockdown. In addition, several proteins involved in EMT were evaluated using Western blot (Fig. S2C).

We also generated A549/shp23 lung cancer cells that stably overexpressed CXCL1 (A549/shp23+OECXCL1). As shown in Fig. 3A−C, CXCL1 significantly reversed the migration inhibition caused by p23 knockdown, as well as the changes in the expression of proteins related to EMT (E-cadherin, N-cadherin, and vimentin) (Fig. 3D). Moreover, similar results were observed *in vivo*. p23 knockdown significantly reduced the number of lung metastatic nodules in NYG mice, and this reduction was completely reversed by CXCL1 overexpression (Fig. 3E−H). These results indicate that p23 promotes the metastasis of lung cancer through the expression of CXCL1.

3.5. p23 regulates the transcriptional expression of CXCL1 rather than affecting its mRNA stability

To further assess the function of p23 in CXCL1 expression, we examined the effect of p23 on *CXCL1* mRNA stability. Although p23 depletion or overexpression positively regulated the basal mRNA levels of endogenous CXCL1, the half-life of *CXCL1* mRNA was not affected by the changes made to p23 (Supporting Information Fig. S3A and S3B), indicating that p23 upregulates CXCL1 expression at the transcriptional level, rather than affecting mRNA stability. Furthermore, luciferase reporter plasmids containing the *CXCL1* promoter region (−874 to +38) were constructed. Indeed, p23 expression dramatically increased CXCL1 luciferase activity (Fig. 4A). Through generating truncated variants of the *CXCL1* promoter, we observed that p23 has an obvious activation effect in the −744 to +38 region of the *CXCL1* promoter (Fig. 4B), which indicated that the binding sites for p23 are located in this region. Thus, a biotin-labeled probe, in accordance with the optimum *CXCL1* promoter (−744 to +38), was used to evaluate p23 binding, with the *CXCL1* promoter (−549 to +38) as a negative control. As expected, pulldown of the *CXCL1* promoter region −744 to +38 from A549 cell nuclear extract visualized p23 protein, whereas no signal was detected in the negative control region (Fig. 4C).

Then the region (−549 to −744 bp) was truncated into 5 fragments to further confirm the binding motif of p23 in the *CXCL1* promoter, including P1 (probe 1): −744 to −703, P2 (probe 2): −707 to −663, P3 (probe 3): −667 to −621, P4 (probe 4): −625 to −579, and P5 (probe 5): −583 to −537. The nucleotide sequences of the CXCL1−EMSA probes are listed in Supporting Information Table S2. The interaction between p23 and the probe was analyzed by EMSA assay with HEK293T cell lysates overexpressing p23. We found that p23 had binding affinities for P1, P2, and P3 (Fig. 4D), indicating that these 3 fragments contained p23 binding motifs. This observation was further validated using an anti-p23 antibody to competitively block binding between p23 and CXCL1 (Fig. 4E). Further Multiple Em for Motif Elicitation (MEME) analysis revealed a 6 bp p23-binding motif from 3 fragments with conserved locations at nucleotides 1C, 2A, 3C, 4T, 5G/T, and 6A (Fig. 4F). Mutation of these motifs completely abolished p23-induced CXCL1 reporter activity (Fig. 4G). These results further confirm the transcriptional regulatory effect of p23 on CXCL1 expression. To further investigate the direct binding of p23 to the *CXCL1* promoter, we conducted an EMSA assay using purified p23 protein. Surprisingly, purified p23 exhibited no binding affinity towards the *CXCL1* promoter (Fig. 4H), suggesting that p23's transcriptional regulation of CXCL1 may not be solely dependent on its direct interaction with the promoter, but rather requires the involvement of other protein factors.

3.6. RBM14 promotes the transcriptional regulation of p23 on CXCL1

To investigate the participants involved in the regulation of CXCL1 by p23, 34 proteins interacting with p23 were identified through Co-IP combined with mass spectrometry, four of which were selected because of their transcriptional function (Fig. 5A).

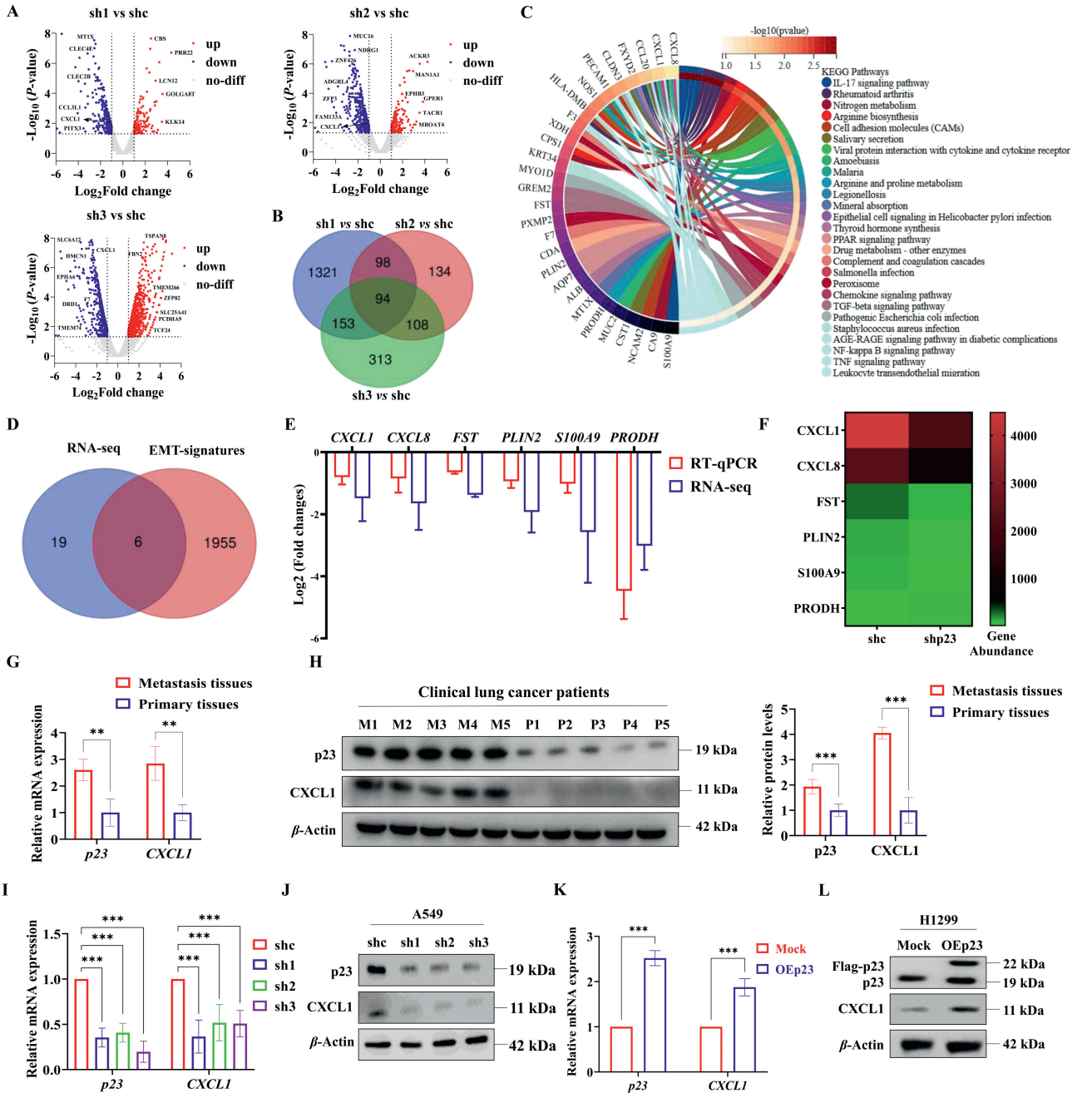

Figure 2 The downstream target gene CXCL1 of p23 was found by RNA-seq sequencing. (A) Volcano maps show three groups of gene changes after p23 knock-down. (B) Venn diagram shows the expression levels of all 94 differential genes in the sample. (C) KEGG pathway enrichment was used to analyze 94 differentially expressed genes after p23 knockdown. (D) Venn diagram shows genes from the KEGG pathway that can be used as EMT signatures. (E) 6 EMT markers were selected to execute qPCR identification. (F) Heat map of the content of 6 EMT genes. (G) Relative mRNA levels of *p23* and *CXCL1* in metastatic and non-metastatic lung cancer tissues, $n = 5$. (H) Representative Western blotting images of p23 and CXCL1 in metastatic and non-metastatic lung cancer tissues, and quantitative analysis were performed using image lab software, $n = 5$. (I) Relative mRNA levels of *CXCL1* after p23 knockdown, $n = 3$. (J) Representative Western blotting images of CXCL1 after p23 knockdown, $n = 3$. (K) Relative mRNA levels of *CXCL1* after p23 overexpression, $n = 3$. (L) Representative Western blotting images of CXCL1 after p23 overexpression, $n = 3$. Results are presented as mean ± SD. $^*P < 0.05$, $^{**}P < 0.01$, $^{***}P < 0.001$ indicates a significant difference between groups.

Co-IP assays further verified their interaction with p23 (Fig. 5B, Supporting Information Fig. S4A), demonstrating the accuracy of the identification results by mass spectrometry. However, only RBM14 was pulled down using a *CXCL1* promoter probe (Fig. 5C, Fig. S4B) and significantly promoted the reporter activity of the optimal CXCL1 promoter enhanced by p23 (Fig. 5D). A similar result was obtained from Western blot analysis (Fig. 5E). Furthermore, we conducted an EMSA to investigate the

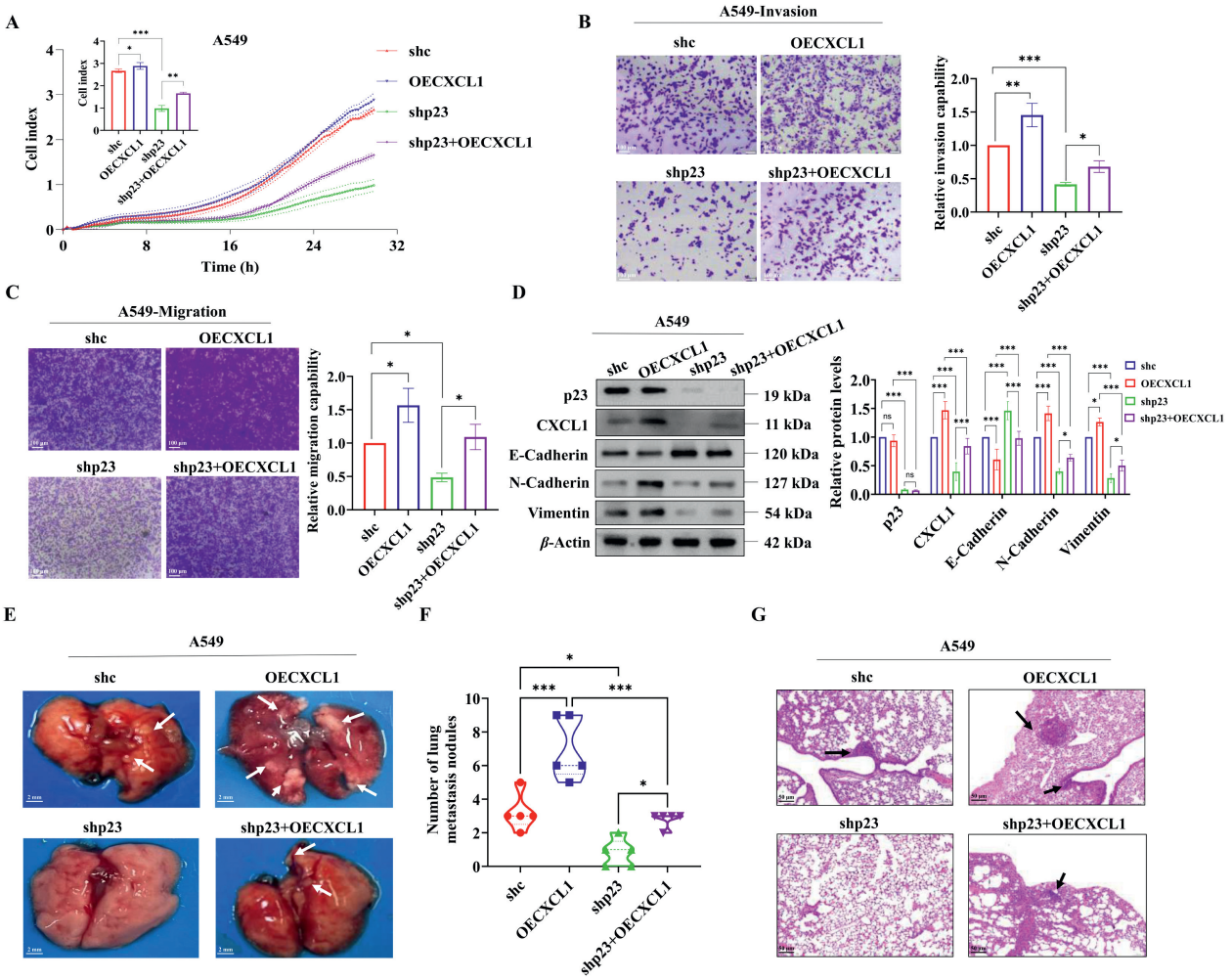

Figure 3 The EMT induced by p23 is partially dependent on CXCL1. (A) The number of migrating cells were determined in real time by xCELLigence, $n = 3$. (B, C) The influence of p23 and CXCL1 on the invasion and migration ability of A549 cells was investigated by the Transwell invasion experiment (B) and migration experiment (C). Scale bar: 100 μm, $n = 3$. (D) Expression changes of invasion and migration proteins N-cadherin, Vimentin, and E-cadherin by Western blotting, and quantitative analysis was performed using image lab software, $n = 3$. (E) Representative lung metastatic nodule images after tail vein injection of four cell lines (A549/wt, A549/OECXCL1, A549/shp23, A549/shp23+OECXCL1). Scale bar: 2 mm, $n = 5$. (F) Statistics of lung metastatic nodule numbers in each group, $n = 5$. (G) Representative H&E staining images for lung metastatic nodules. Scale bars: 50 μm, $n = 3$. The results are presented as the mean ± SD. ns, no significance; $^{*}P < 0.05$, $^{**}P < 0.01$, $^{***}P < 0.001$ signifies a significant difference between the groups.

binding activity of purified p23 and RBM14 proteins to the CXCL1 promoter. As expected, pure p23 or RBM14 proteins individually did not directly bind to the CXCL1 promoter; however, their complexes demonstrated binding activity (Fig. 5F). These results suggest that the interaction between p23 and RBM14 played a crucial role in the regulation of CXCL1 expression.

We explored the mechanisms underlying the role of the p23/RBM14 protein complex in the transcriptional regulation of CXCL1. No reciprocal influence was observed between p23 and RBM14 on protein and mRNA expression levels (Fig. S4C−S4F). Subsequently, we modulated intracellular complex production to elucidate the regulation of the p23−RBM14 complex on CXCL1. As shown in Fig. 5G, the overexpression of the RBM14 protein with an HA tag in the A549 cell line was used for IP experiments. After p23 was knocked down or overexpressed, the amount of RBM14 detected by IP decreased or increased, respectively. When p23 was knocked down and then supplemented, the amount of RBM14 caught by IP returned to the same level as that of the control group. Similarly, in the A549 cell line overexpressing p23 with a Flag tag, knocking down or overexpressing RBM14 also decreased or increased the amount of p23 obtained by IP, and when RBM14 was knocked down and replenished, the p23 detected by IP returned to control group levels (Fig. 5H). Similarly, the binding activity of p23 and RBM14 to the *CXCL1* promoter probe was significantly affected by the disruption of the p23/RBM14 complex. To achieve this, we constructed cell lines in which either p23 or RBM14 was knocked down. As shown in Fig. 5I, the third lane shows that RBM14 overexpression activated CXCL1 transcription compared with the first lane. This is likely because RBM14, a known transcriptional coactivator, can assist not only p23, but also other transcription factors in regulating CXCL1 transcription. As shown in the second and fourth lanes, regardless of RBM14 overexpression, p23 knockdown weakened CXCL1 activation. Similarly, Fig. 5J shows that compared to the

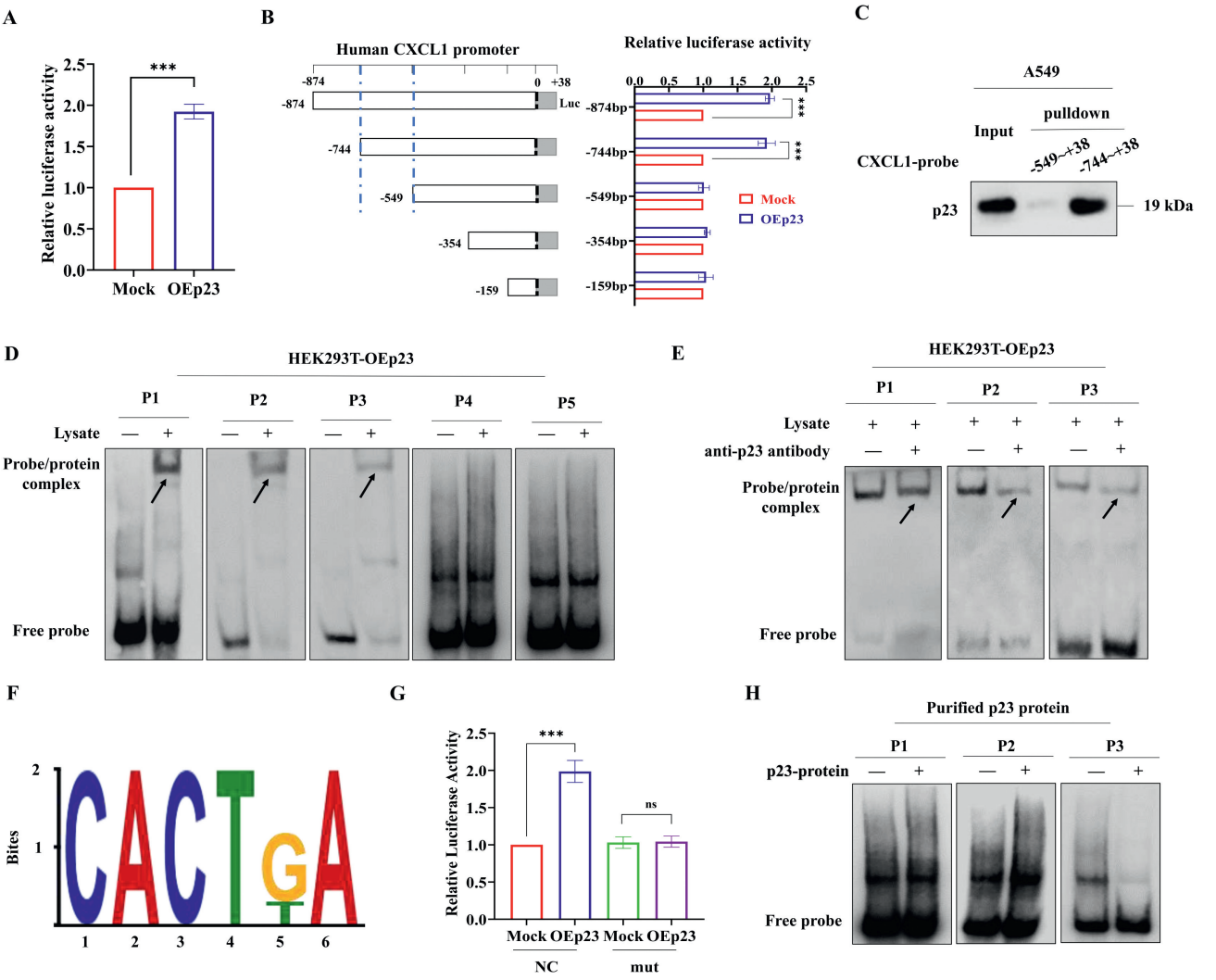

Figure 4 p23 regulates the expression of CXCL1 at the transcriptional level, but does not affect its mRNA stability. (A, B) Dual-luciferase reporter gene detection of CXCL1 reporter gene with the best promoter region (A) and truncated variant (B), $n = 3$. (C) Pulldown assay of the binding of biotin-labeled CXCL1 promoter DNA (from −549 to +38 and from −744 to +38) and p23, $n = 3$. (D) EMSA assay of the binding of 5 fragments of CXCL1 and p23; P1 to P5: 5 EMSA fragments of CXCL1 promoter, $n = 3$. (E) Competitive binding analysis EMSA by using anti-p23 antibody, $n = 3$. (F) The binding motif of p23 and CXCL1. (G) Changes in the activity of p23 to CXCL1 dual-luciferase reporter gene after mutation of binding motif, $n = 3$. (H) EMSA experiment of the binding of p23 pure protein and CXCL1 probe, $n = 3$. Results are presented as mean ± SD. ns, no significance; $^{*}P < 0.05$, $^{**}P < 0.01$, $^{***}P < 0.001$ indicates a significant difference between groups.

first lane, p23 overexpression in the third lane leads to CXCL1 transcriptional activation. However, further RBM14 knockdown weakened CXCL1 activation regardless of whether p23 was overexpressed. These results illustrate the impact of disrupting the p23−RBM14 complex on CXCL1 transcription at the p23 binding site in the *CXCL1* promoter region (−744 to +38 bp). This is consistent with the dual-luciferase reporter assay results for the −874 to +38 bp region (Fig. S4M and S4Q). However, when p23 did not bind to the −159 to +38 bp, −354 to +38 bp, or −549 to +38 bp regions of the *CXCL1* promoter, RBM14 overexpression slightly activated CXCL1 transcription. By contrast, p23 knockdown did not affect transcriptional activation in these cases (Fig. S4J−S4L). Conversely, while p23 overexpression did not activate CXCL1 transcription, RBM14 knockdown partially affected transcriptional activation (Fig. S4N−S4P). In summary, when the p23−RBM14 complex is disrupted by the knockdown of either protein, CXCL1 transcriptional regulation is weakened. These results suggest that the interaction between p23 and RBM14 played a critical role in regulating CXCL1 expression. The DNA pulldown assay using a CXCL1 probe in A549 cells further demonstrated that the knockdown of either p23 or RBM14 resulted in a corresponding reduction in the amount of the other protein being captured by the CXCL1 probe (Fig. 5K and L).

Since p23 is known as a classical chaperone protein of HSP90, we also examined HSP90's effect on the p23-mediated transcriptional regulation of CXCL1. As shown in Fig. S4G, the luciferase assay results indicated that HSP90 alone could not regulate CXCL1 nor could it enhance p23's regulation of CXCL1 when overexpressed with p23. Additionally, we tested whether p23's transcriptional regulation of CXCL1 depends on HSP90.

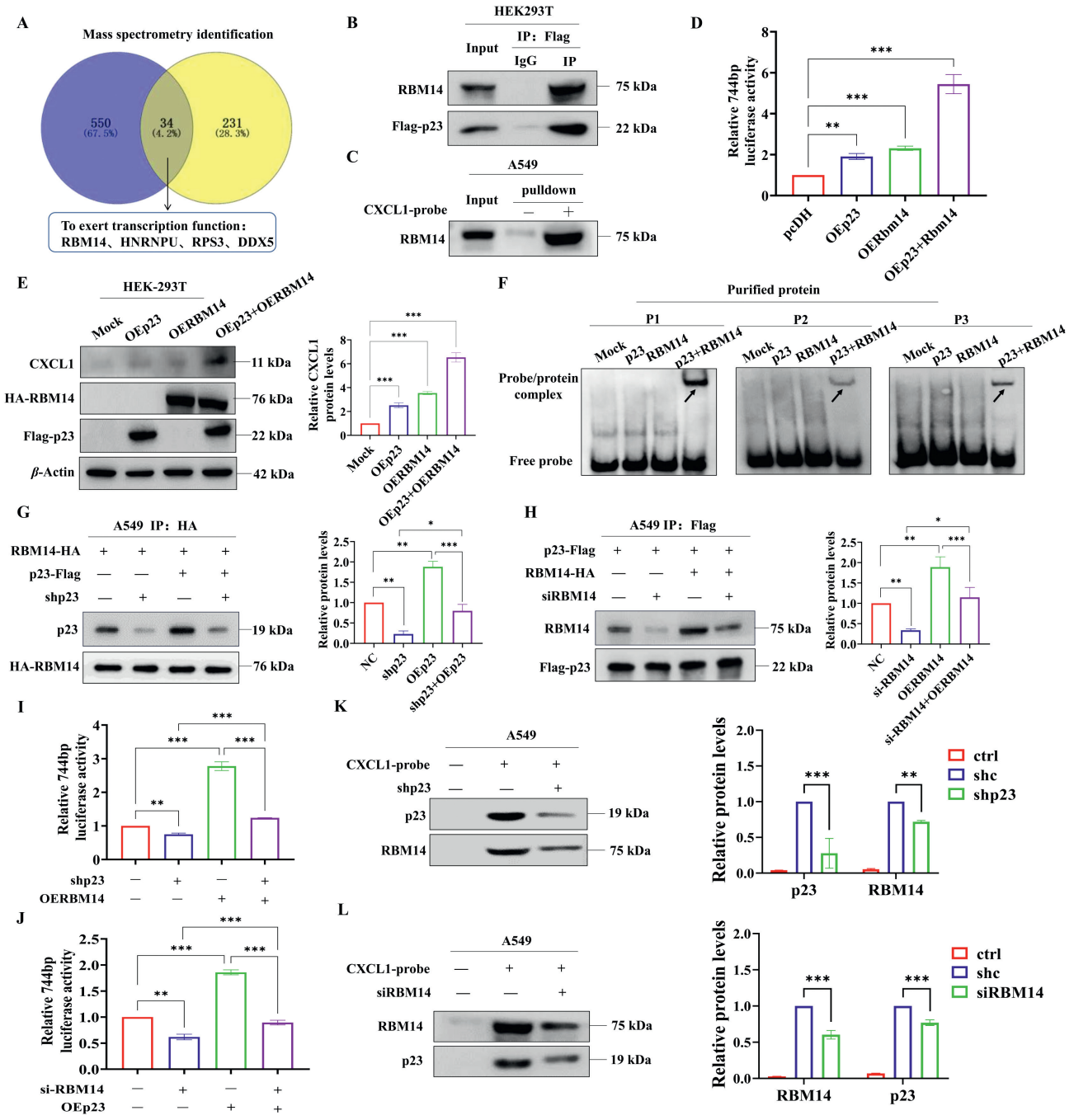

Figure 5 RBM14 promotes the transcriptional regulation of p23 on CXCL1. (A) Twice identifying the results by mass spectrometry and selecting the protein with transcription activity. (B) Co-IP was used to verify the interaction with p23, $n = 3$. (C) Pulldown fishing with CXCL1 promoter probe, $n = 3$. (D) Dual-luciferase reporter gene assay proved that RBM14 can promote the transcriptional regulation of p23 on CXCL1, $n = 3$. (E) Western blotting verified that RBM14 promoted the transcriptional regulation of p23 on CXCL1, $n = 3$. (F) The transcription of CXCL1 can only be started when the coexistence of p23 and RBM14 pure protein was verified by the EMSA experiment, $n = 3$. (G, H) Co-IP revealed the complex of p23 and RBM14 was embellished, $n = 3$. (I) Dual-luciferase reporter gene assay proved that knocking down p23 would reduce the exciting effect of RBM14 on CXCL1, $n = 3$. (J) The dual-luciferase reporter gene assay confirmed that if RBM14 was knocking down, p23 would reduce the exciting effect of CXCL1, $n = 3$. (K) Pulldown assay proved that when p23 was knocked down, RBM14 caught in the CXCL1 promoter region would decrease accordingly, $n = 3$. (L) Pulldown assay proved that when RBM14 was knocked down, p23 caught in the CXCL1 promoter region would decrease accordingly, $n = 3$. Results are presented as mean ± SD. $^{*}P < 0.05$, $^{**}P < 0.01$, $^{***}P < 0.001$ indicates a significant difference between groups.

Using a p23 plasmid with a mutation at the interaction site between p23 and HSP90 (W106A/D108A) in HEK293T cells, luciferase results showed that the mutated p23 retained its transcriptional activity on CXCL1 (Fig. S4H and S4I). Therefore, p23's transcriptional regulation of CXCL1 is independent of HSP90 expression. In conclusion, these results demonstrate that the formation of the p23/RBM14 protein complex plays a pivotal role in mediating p23-induced CXCL1 expression.

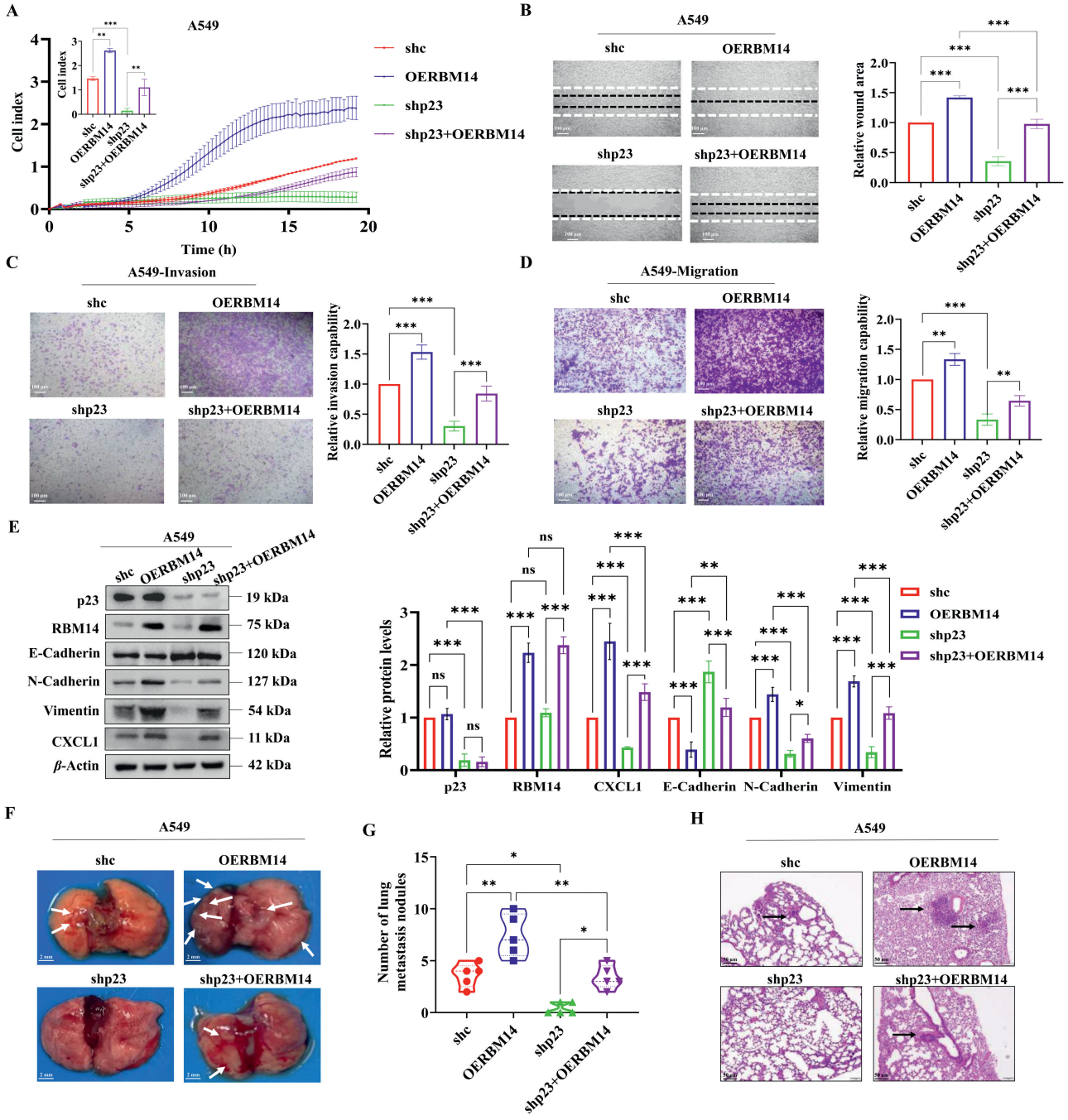

Figure 6 The influence of p23 on EMT is partially dependent on RBM14. (A) xCELLigence determined the number of migrating cells in real-time, $n = 3$. (B–D) Wound-healing assay (B), invasion assay (C) and migration assay (D) of A549 cells after RBM14 overexpressing and p23 knocking down. Scale bar: 100 μm, $n = 3$. (E) The changes in the expression of the invasion and migration proteins E-cadherin, N-cadherin, Vimentin and their quantitative graphs, $n = 3$. (F) Representative lung metastatic nodule images after tail vein injection of four cell lines (A549/shc, A549/OERBM14, A549/shp23, A549/shp23+OERBM14). Scale bar: 2 mm, $n = 5$. (G) Statistics of lung metastatic nodule numbers in each group, $n = 5$. (H) Representative H&E staining images for lung metastatic nodules. Scale bar: 50 μm, $n = 3$. Data are presented as means ± SD. ns, no significance; $^*P < 0.05$, $^{**}P < 0.01$, $^{***}P < 0.001$ denotes a significant difference between groups.

3.7. *Influence of p23 on EMT is partially dependent on RBM14*

To explore whether the EMT induced by p23 was RBM14-dependent, we constructed 4 stable cell lines using a lentivirus infection system: A549/shc, A549/OERBM14, A549/shp23, and A549/shp23+OERBM14. *In vitro*, the xCELLigence assay was used to monitor cell migration in real time (Fig. 6A). This result suggests that RBM14 could promote the EMT phenotype, but when p23 was knocked down simultaneously, the EMT phenotype was slightly reduced. Furthermore, wound healing (Fig. 6B), invasion (Fig. 6C), and migration (Fig. 6D) experiments were carried out and similar conclusions were reached. Changes in N-cadherin, E-cadherin, and vimentin protein levels were evaluated using Western blot (Fig. 6E), which also showed that p23 promoted the EMT phenotype in an RBM14-dependent manner. *In vivo*, the quantity of pulmonary metastatic nodules (Fig. 6F and G) and H&E staining of pulmonary metastatic nodules (Fig. 6H) were assessed by tail vein injection of four stably transfected cell lines, A549/shc, A549/shp23, A549/OERBM14 and A549/shp23+OERBM14. From these results, we can conclude that EMT induced by p23 is partially dependent on RBM14.

4. Discussion

Lung cancer is the most common and deadly malignant tumor in China even around the world, and the outcomes of treatment are poor[43]. The metastasis of lung cancer represents a malignant manifestation and biological characteristic and serves as the primary cause of mortality in patients with this disease[44]. The metastatic nature of cancer leads tumor cells to spread from the primary site through the blood and lymphatic system to distant tissues beyond the lungs[45], resulting in a substantial reduction in the efficacy of conventional therapies. Consequently, impeding lung cancer metastasis is of paramount importance for extending patient survival, improving overall prognosis, enhancing quality of life, and ameliorating treatment outcomes[46]. Metastasis of lung cancer is a multifaceted and complex process involving a large number of stages, steps, genes, and factors. Therefore, a major area of research in the effort to overcome lung cancer has been to elucidate the molecular mechanisms underlying lung cancer invasion and metastasis and to identify molecular targets to reverse or prevent these processes. In this study, we identified a novel pathway that regulates lung cancer metastasis, that is RBM14 assists p23 in enhancing the transcription activity of CXCL1, thereby promoting tumor metastasis. We provide a theoretical basis for the clinical treatment of lung cancer and for the screening of potential anti-metastatic agents from the perspective of inhibiting lung cancer invasion and metastasis.

PTGES3 (p23) is a molecular chaperone protein and potential oncogene[22-24]. Previous studies[23] showed that p23 is highly expressed in lung adenocarcinoma, and its overexpression is associated with short overall survival and poor prognosis in patients with lung cancer. The relation between PTGES3 and EMT was first reported to indicate that p23 can promote the metastasis of lung cancer[47]. It is not yet known how it works. Our results indicate that p23 is important in the promotion of EMT in human lung cancer, both *in vivo* and *in vitro*. Our study demonstrated that the primary mechanism through which p23 promotes EMT is its regulation of CXCL1 expression *via* binding to the promoter region of CXCL1.

As critical regulators of biological processes[48], the functions of proteins are often manifested through their interactions with other proteins[49]. In order to understand and prevent disease, target the treatment of polygenic disorders, and elucidate the molecular mechanisms underlying complex biological phenomena, the study of protein−protein interactions is of immense importance[50,51]. In this study, we showed that p23 acts as a transcription factor that binds indirectly to the promoter region of CXCL1, suggesting the involvement of potential cofactors that facilitate p23-mediated transcription. We identified RBM14 as this cofactor using mass spectrometry combined with Co-IP and DNA pulldown experiments.

RBM14 functions as a transcriptional coactivator, also known as CoActivator Activator (CoAA). RBM14 shows widespread expression in embryonic tissues and plays a critical role in regulating early embryonic development[52,53]. RBM14 is significantly upregulated in tumors, promoting tumor proliferation and migration[38,54]. However, the precise molecular mechanism remains unclear. It has been demonstrated that RBM14 enhances transcription through the action of other coactivators, such as NCOA6 and CITED1[41]. RBM14 may also act as a transcription coactivator for other transcription factors to regulate CXCL1, thus activating CXCL1 transcription in the promoter region fragment where p23 is not bound to CXCL1. This is undeniable and requires further exploration. Our experiment is the first to demonstrate that RBM14, as a transcriptional coactivator of p23, assists p23 in the transcriptional regulation of CXCL1 and underscores that both must form a complex to function effectively, making both indispensable. In the presence of RBM14, the transcriptional regulation of p23 on CXCL1 was greatly enhanced.

While our previous study reported that p23 regulates COX-2 expression[35], we found that p23 affected lung cancer metastasis, even after COX-2 knockout. This suggests that p23 influences tumor metastasis through additional pathways. In the present study, we demonstrated that the regulation of CXCL1 and the induction of lung cancer cell metastasis by the p23−RBM14 complex are independent of COX-2. First, we examined the expression of COX-2, CXCL1, and p23 in human lung fibroblasts and various lung cancer cell lines, with the results presented in Supporting Information Fig. S5A. Furthermore, the expression levels of RBM14, and COX-2 were significantly higher in lung cancer that had spread than in those that had not (Fig. S5B), with CXCL1 showing the most pronounced increase (Fig. 2H). To further explore the relation between COX-2 and the effect of p23 on lung cancer cell migration and invasion, we generated a COX-2 knockout cell line (A549/KOCOX-2) (Fig. S5C). The migration and invasion abilities of A549/KOCOX-2 cells were further reduced following p23 knockout (Fig. S5D−S5G). Scratch assays demonstrated that the loss of endogenous p23 inhibited the migration of A549 lung cancer cells, even in COX-2 knockout tumor cells (Fig. S5D). Similar results were observed in the Transwell invasion (Fig. S5E) and migration assays (Fig. S5F). In addition, proteins associated with EMT, including N-cadherin, E-cadherin, and vimentin, exhibited corresponding changes following the p23 knockout (Fig. S5G). Additionally, we investigated whether the mechanism of CXCL1 expression regulation after p23 and RBM14 form a complex is influenced by COX-2. As shown in Fig. S5H and S5I, in the A549/KOCOX-2 cell line, the CXCL1 promoter region can bind to p23 and RBM14, respectively. However, when one of them is knocked down, the ability of the CXCL1 promoter region to bind to other proteins is weakened. These findings further support the notion that the p23/RBM14 axis regulates EMT in lung cancer independent of COX-2.

5. Conclusions

In this study, we discovered that RBM14 forms a complex with p23, thereby augmenting the transcriptional regulation of p23 on CXCL1 expression. When there is a decrease or absence of expression of either component, the formation of the complex is reduced, resulting in the inhibition of CXCL1 transcriptional expression, which subsequently weakens cellular invasion and migration abilities. Our findings suggest that RBM14 serves as a coactivator of p23 to promote EMT in lung cancer.

Acknowledgements

The authors thank the National Natural Science Foundation of China (82225048 and 82004089), "1+X" Research Project of the Second Hospital of Dalian Medical University (LYYH2024002, China), and Dalian Medical University Interdisciplinary Research Cooperation Project Team Funding (JCHZ2023011, China) for financial support.

Author contributions

Wen Zhang: Writing − review & editing, Writing − original draft, Supervision, Software, Resources, Methodology, Investigation, Formal analysis, Data curation. Yulin Peng: Validation, Software, Conceptualization. Meirong Zhou: Methodology, Investigation, Data curation, Conceptualization. Lei Qian: Software, Investigation, Conceptualization. Yilin Che: Resources. Junlin Chen: Software, Data curation. Wenhao Zhang: Supervision, Software. Chengjian He: Software, Data curation. Minghang Qi: Software. Manman Tian: Software. Xiangge Tian: Supervision, Software. Yan Tian: Supervision. Xiaohong Shu: Investigation. Sa Deng: Software. Yan Wang: Software. Xiaokui Huo: Validation. Zhenlong Yu: Methodology, Investigation, Data curation, Conceptualization. Xiaochi Ma: Investigation, Conceptualization.

Conflicts of interest

The authors declare no competing interests.

Appendix A. Supporting information

Supporting information to this article can be found online at https://doi.org/10.1016/j.apsb.2025.03.048.

References

1. Thai AA, Solomon BJ, Sequist LV, Gainor JF, Heist RS. Lung cancer. *Lancet* 2021;**398**:535−54.
2. Schabath MB, Cote ML. Cancer progress and priorities: lung cancer. *Cancer Epidemiol Biomarkers Prev* 2019;**28**:1563−79.
3. Nasim F, Sabath BF, Eapen GA. Lung cancer. *Med Clin* 2019;**103**: 463−73.
4. Hirsch FR, Scagliotti GV, Mulshine JL, Kwon R, Curran WJ, Wu YL, et al. Lung cancer: current therapies and new targeted treatments. *Lancet* 2017;**389**:299−311.
5. Wu SG, Shih JY. Management of acquired resistance to EGFR TKI-targeted therapy in advanced non-small cell lung cancer. *Mol Cancer* 2018;**17**:38.
6. Zeng H, Chen W, Zheng R, Zhang S, Ji JS, Zou X, et al. Changing cancer survival in China during 2003−15: a pooled analysis of 17 population-based cancer registries. *Lancet Global Health* 2018;**6**: e555−67.
7. Robert J. Biology of cancer metastasis. *Bulletin Du Cancer* 2013;**100**: 333−42.
8. Fares J, Fares MY, Khachfe HH, Salhab HA, Fares Y. Molecular principles of metastasis: a hallmark of cancer revisited. *Signal Transduct Targeted Ther* 2020;**5**:28.
9. Pan G, Liu Y, Shang L, Zhou F, Yang S. EMT-associated microRNAs and their roles in cancer stemness and drug resistance. *Cancer Commun* 2021;**41**:199−217.
10. Suarez-Carmona M, Lesage J, Cataldo D, Gilles C. EMT and inflammation: inseparable actors of cancer progression. *Mol Oncol* 2017;**11**:805−23.
11. Korbecki J, Barczak K, Gutowska I, Chlubek D, Baranowska-Bosiacka I. CXCL1: gene, promoter, regulation of expression, mRNA stability, regulation of activity in the intercellular space. *Int J Mol Sci* 2022;**23**:792.
12. Korbecki J, Gąssowska-Dobrowolska M, Wójcik J, Szatkowska I, Barczak K, Chlubek M, et al. The importance of CXCL1 in physiology and noncancerous diseases of bone, bone marrow, muscle and the nervous system. *Int J Mol Sci* 2022;**23**:4205.
13. Wang N, Liu W, Zheng Y, Wang S, Yang B, Li M, et al. CXCL1 derived from tumor-associated macrophages promotes breast cancer metastasis *via* activating NF-κB/SOX4 signaling. *Cell Death Dis* 2018;**9**:880.
14. Taki M, Abiko K, Baba T, Hamanishi J, Yamaguchi K, Murakami R, et al. Snail promotes ovarian cancer progression by recruiting myeloid-derived suppressor cells *via* CXCR2 ligand upregulation. *Nat Commun* 2018;**9**:1685.
15. Saintigny P, Massarelli E, Lin S, Ahn YH, Chen Y, Goswami S, et al. CXCR2 expression in tumor cells is a poor prognostic factor and promotes invasion and metastasis in lung adenocarcinoma. *Cancer Res* 2013;**73**:571−82.
16. Zhao J, Ou B, Feng H, Wang P, Yin S, Zhu C, et al. Overexpression of CXCR2 predicts poor prognosis in patients with colorectal cancer. *Oncotarget* 2017;**8**:28442−54.
17. Chen L, Fan J, Chen H, Meng Z, Chen Z, Wang P, et al. The IL-8/CXCR1 axis is associated with cancer stem cell-like properties and correlates with clinical prognosis in human pancreatic cancer cases. *Sci Rep* 2014;**4**:5911.
18. Sanford DE, Belt BA, Panni RZ, Mayer A, Deshpande AD, Carpenter D, et al. Inflammatory monocyte mobilization decreases patient survival in pancreatic cancer: a role for targeting the CCL2/CCR2 axis. *Clin Cancer Res* 2013;**19**:3404−15.
19. Lee CW, Chiang YC, Yu PA, Peng KT, Chi MC, Lee MH, et al. A role of CXCL1 drives osteosarcoma lung metastasis *via* VCAM-1 production. *Front Oncol* 2021;**11**:735277.
20. Cha JY, Ermawati N, Jung MH, Su'udi M, Kim KY, Kim JY, et al. Characterization of orchardgrass p23, a flowering plant Hsp90 cohort protein. *Cell Stress Chaperones* 2009;**14**:233−43.
21. Zhang Z, Sullivan W, Felts SJ, Prasad BD, Toft DO, Krishna P. Characterization of plant p23-like proteins for their co-chaperone activities. *Cell Stress Chaperones* 2010;**15**:703−15.
22. Adekeye A, Agarwal D, Nayak A, Tchou J. PTGES3 is a putative prognostic marker in breast cancer. *J Surg Res* 2022;**271**:154−62.
23. Gao P, Zou K, Xiao L, Zhou H, Xu X, Zeng Z, et al. High expression of PTGES3 is an independent predictive poor prognostic biomarker and correlates with immune infiltrates in lung adenocarcinoma. *Int Immunopharmacol* 2022;**110**:108954.
24. He Y, Peng S, Wang J, Chen H, Cong X, Chen A, et al. Ailanthone targets p23 to overcome MDV3100 resistance in castration-resistant prostate cancer. *Nat Commun* 2016;**7**:13122.
25. Elmore LW, Forsythe R, Forsythe H, Bright AT, Nasim S, Endo K, et al. Overexpression of telomerase-associated chaperone proteins in prostatic intraepithelial neoplasia and carcinomas. *Oncol Rep* 2008;**20**: 613−7.
26. Reebye V, Querol Cano L, Lavery DN, Brooke GN, Powell SM, Chotai D, et al. Role of the HSP90-associated cochaperone p23 in

enhancing activity of the androgen receptor and significance for prostate cancer. *Mol Endocrinol* 2012;**26**:1694−706.
27. Simpson NE, Lambert WM, Watkins R, Giashuddin S, Huang SJ, Oxelmark E, et al. High levels of Hsp90 cochaperone p23 promote tumor progression and poor prognosis in breast cancer by increasing lymph node metastases and drug resistance. *Cancer Res* 2010;**70**:8446−56.
28. Fang Y, Fliss AE, Rao J, Caplan AJ. SBA1 encodes a yeast hsp90 cochaperone that is homologous to vertebrate p23 proteins. *Mol Cell Biol* 1998;**18**:3727−34.
29. Sullivan W, Stensgard B, Caucutt G, Bartha B, McMahon N, Alnemri ES, et al. Nucleotides and two functional states of hsp90. *J Biol Chem* 1997;**272**:8007−12.
30. Knoblauch R, Garabedian MJ. Role for Hsp90-associated cochaperone p23 in estrogen receptor signal transduction. *Mol Cell Biol* 1999;**19**: 3748−59.
31. Thomas M, Harrell JM, Morishima Y, Peng H-M, Pratt WB, Lieberman AP. Pharmacologic and genetic inhibition of hsp90-dependent trafficking reduces aggregation and promotes degradation of the expanded glutamine androgen receptor without stress protein induction. *Hum Mol Genet* 2006;**15**:1876−83.
32. Holt SE, Aisner DL, Baur J, Tesmer VM, Dy M, Ouellette M, et al. Functional requirement of p23 and Hsp90 in telomerase complexes. *Genes Dev* 1999;**13**:817−26.
33. Wu H, Hyun J, Martinez-Yamout MA, Park SJ, Dyson HJ. Characterization of an Hsp90-independent interaction between co-chaperone p23 and transcription factor p53. *Biochemistry* 2018;**57**:935−44.
34. Pappas B, Yang Y, Wang Y, Kim K, Chung HJ, Cheung M, et al. p23 protects the human aryl hydrocarbon receptor from degradation *via* a heat shock protein 90-independent mechanism. *Biochem Pharmacol* 2018;**152**:34−44.
35. Gao ZYYPJ. The p23 co-chaperone is a succinate-activated COX-2. *Sci Adv* 2023;**9**:eade0387.
36. Iwasaki T, Chin WW, Ko L. Identification and characterization of RRM-containing coactivator activator (CoAA) as TRBP-interacting protein, and its splice variant as a coactivator modulator (CoAM). *J Biol Chem* 2001;**276**:33375−83.
37. Shiratsuchi G, Takaoka K, Ashikawa T, Hamada H, Kitagawa D. RBM14 prevents assembly of centriolar protein complexes and maintains mitotic spindle integrity. *EMBO J* 2015;**34**:97−114.
38. Hu J, Yang L, Peng X, Mao M, Liu X, Song J, et al. METTL3 promotes m6A hypermethylation of RBM14 *via* YTHDF1 leading to the progression of hepatocellular carcinoma. *Hum Cell* 2022;**35**:1838−55.
39. Zhang S, Li Q, Yuan H, Ren L, Liang X, Li S, et al. Solute carrier family 35 member F2 regulates cisplatin resistance and promotes malignant progression of pancreatic cancer by regulating RNA binding motif protein 14. *JAMA Oncol* 2022;**2022**:5091154.
40. Kai M. Roles of RNA-binding proteins in DNA damage response. *Int J Mol Sci* 2016;**17**:310.
41. Simon NE, Yuan M, Kai M. RNA-binding protein RBM14 regulates dissociation and association of non-homologous end joining proteins. *Cell Cycle* 2017;**16**:1175−80.
42. Najjar YG, Rayman P, Jia X, Pavicic PG, Rini BI, Tannenbaum C, et al. Myeloid-derived suppressor cell subset accumulation in renal cell carcinoma parenchyma is associated with intratumoral expression of IL1β, IL8, CXCL5, and Mip-1α. *Clin Cancer Res* 2017;**23**: 2346−55.
43. Sung H, Ferlay J, Siegel RL, Laversanne M, Soerjomataram I, Jemal A, et al. Global cancer statistics 2020: GLOBOCAN estimates of incidence and mortality worldwide for 36 cancers in 185 countries. *CA Cancer J Clin* 2021;**71**:209−49.
44. Xia HW, Zhang ZQ, Yuan J, Niu QL. Human RECQL5 promotes metastasis and resistance to cisplatin in non-small cell lung cancer. *Life Sci* 2021;**265**:118768.
45. Chaffer CL, Weinberg RA. A perspective on cancer cell metastasis. *Science* 2011;**331**:1559−64.
46. Bakir B, Chiarella AM, Pitarresi JR, Rustgi AK. EMT, MET, plasticity, and tumor metastasis. *Trends Cell Biol* 2020;**30**:764−76.
47. Fu Q, Wang W, Zhou T, Yang Y. Emerging roles of NudC family: from molecular regulation to clinical implications. *Sci China Life Sci* 2016; **59**:455−62.
48. Mazmanian K, Sargsyan K, Lim C. How the local environment of functional sites regulates protein function. *J Am Chem Soc* 2020;**142**: 9861−71.
49. Wang T, Yang N, Liang C, Xu H, An Y, Xiao S, et al. Detecting protein−protein interaction based on protein fragment complementation Assay. *Curr Protein Pept Sci* 2020;**21**:598−610.
50. Athanasios A, Charalampos V, Vasileios T, Ashraf GM. Protein−-protein interaction (PPI) network: recent advances in drug discovery. *Curr Drug Metabol* 2017;**18**:5−10.
51. Hu X, Feng C, Ling T, Chen M. Deep learning frameworks for protein-protein interaction prediction. *Comput Struct Biotechnol J* 2022;**20**:3223−33.
52. Yang Z, Sui Y, Xiong S, Liour SS, Phillips AC, Ko L. Switched alternative splicing of oncogene CoAA during embryonal carcinoma stem cell differentiation. *Nucleic Acids Res* 2007;**35**:1919−32.
53. Brooks YS, Wang G, Yang Z, Smith KK, Bieberich E, Ko L. Functional pre- mRNA trans-splicing of coactivator CoAA and corepressor RBM4 during stem/progenitor cell differentiation. *J Biol Chem* 2009; **284**:18033−46.
54. Sui Y, Yang Z, Xiong S, Zhang L, Blanchard KL, Peiper SC, et al. Gene amplification and associated loss of 5′ regulatory sequences of CoAA in human cancers. *Oncogene* 2006;**26**:822−35.